International Journal of Nanomedicine

Dovepress
open access to scientific and medical research

Open Access Full Text Article

ORIGINAL RESEARCH

Label-Free, Smartphone-Based, and Sensitive Nano-Structural Liquid Crystal Aligned by Ceramic Silicon Compound–Constructed DMOAP-Based Biosensor for the Detection of Urine Albumin

This article was published in the following Dove Press journal:
International Journal of Nanomedicine

Er-Yuan Chuang[1]
Ping-Yuan Lin[1]
Po-Feng Wang[1]
Tsung-Rong Kuo[1]
Chih-Hwa Chen[1–4]
Yankuba B Manga[1]
Yu-Cheng Hsiao[1,5]

[1]Graduate Institute of Biomedical Optomechatronics; Graduate Institute of Nanomedicine and Medical Engineering; International PhD Program in Biomedical Engineering; Graduate Institute of Biomedical Materials and Tissue Engineering; School of Biomedical Engineering; College of Biomedical Engineering, Taipei Medical University, Taipei, Taiwan; [2]Department of Orthopedics, Taipei Medical University-Shuang Ho Hospital, New Taipei City, Taiwan; [3]School of Medicine, College of Medicine, Taipei Medical University, Taipei, Taiwan; [4]Research Center of Biomedical Device, Taipei Medical University, Taipei, Taiwan; [5]Cell Physiology and Molecular Image Research Center, Taipei Medical University–Wan Fang Hospital, Taipei, Taiwan

Introduction: The sensitive interfacial interaction of liquid crystals (LC) holds potential for precision biosensors. In the past, the developments of LC biosensors were limited by the complicated manufacturing process, which hinders commercialization and wider applications of such devices. In this report, we demonstrate the first nano-structural polymeric stabilized-cholesteric LC (PSCLC) thin films to be a new label-free biosensing technology.

Methods: The transmission spectra of PSCLC devices were measured by the fiber-optic spectrometer with high-resolution. In addition, a smartphone was set on the stage, and the camera of smartphone was placed and aligned with a set of lenses embedded in the designed stage. To decrease the chromatic and spherical aberrations, an achromatic lens set composition, consisting of both dual-convex lens and concave-plane lens, was applied for measuring and imaging the PSCLC texture. The average and the estimated standard deviation (SD) were used to present quantitative experimental results. The test BSA was immobilized and fulfilled by the ceramic silicon-constructed DMOAP-coated glass in aqueous BSA solutions at 1 mg/mL, 1 μg/mL, and 1 ng/mL.

Results: The fabrication process of PSCLC is much simplified compared to previous LC biosensors. The color of PSCLC biosensor altered with the BSA concentration, making detection result easy to read. The detection limit of 1 ng/mL is achieved for label-free PSCLC biosensor. The PSCLC biosensor was able to successfully detect due to the albumin concentration's alteration, with a linear range of 1 ng/mL–2 mg/mL. Thus, the label-free-proposed design-integrated nanoscale PSCLCs smartphone-based biosensor could successfully detect BSA in a preclinical urine sample.

Conclusion: Finally, we propose a design to integrate the PSCLC biosensor with a smartphone. The PSCLC owns potential for high performance, low cost for detecting various disease biomarkers in home use. Owing to its great potential for high performance and low cost, the PSCLC biosensors can be used as a label-free point-of-care for detecting various disease biomarkers for patients in care homes.

Keywords: polymer-stabilized cholesteric liquid crystal, ceramic silicon compound, trimethoxysilyl, constructed DMOAP, label-free, biosensor, point-of-care, bovine serum albumin

Correspondence: Yu-Cheng Hsiao
Graduate Institute of Biomedical Optomechatronics, College of Biomedical Engineering, Taipei Medical University, Taipei, 11031, Taiwan
Tel +886-2-27361661
Email ychsioa@tmu.edu.tw

Introduction

Liquid crystal (LC)-constructed optical biosensor is being discovered to be extremely auspicious to detect aqueous biological samples due to their simplicity in

optical detecting, cost-effectiveness, and the elimination of the need for labeling bio-species with optical dyes. Besides the LC biosensors invention by Dr Abbott in 2001,[1] they have become an important sensing technology.[2–4] This LC biosensor invention uses biomolecules immobilized on a substrate to induce the vertical-to-planar reorientation of LCs molecules to assist its high sensitivity. However, this kind of LCs biosensors is in a black and white display, lacking color indication. The cholesteric liquid crystals (CLCs) are one kind of LCs where the molecules of LCs are brought into line with each other together in a broad and lengthy axis of the molecule. In the CLCs phase, the molecules of LCs twist to generate self-ordered assemblies with a Nano helical arrangement (liked photonic crystals). It has been well recognized that Nano-structural CLCs have an exclusive optical feature, Bragg reflection, due to their helical geometric-structures. Investigated by Hsiao et al,[5] the CLCs biosensor was proposed as a highly sensitive color-indicating quantitative biosensor. However, the low stability issue was discovered for the CLCs biosensors. Thus, the subsequently rubbing of CLCs when the cells are homeotropically coated with ceramic silicon-constructed N,N-dimethyl-n-octadecyl-3-aminopropyltrimethoxysilyl chloride (DMOAP) aligns the CLCs perpendicular to the interface. Nano-structural polymeric stabilized-cholesteric liquid crystals (PSCLCs) are CLCs molecules stabilized by a polymer network to make them more stable and thinner. Unfortunately, to the best of our knowledge, no previous investigation discussing the detail the usage of ceramic silicon-constructed DMOAP combining biomolecules on elements of nano-structural PSCLCs for biological/optical/in-home-healthcare applications at a significant scale.

Further, biomarkers, such as Albumin in urine samples, can be explored and used to detect chronic kidney disease (CKD). CKD is a disorder were patient gradually loses their kidney ability to function over time. Globally, CKD is a significant public health issue,[6] which is rank 12th most common cause of death each year due to lack of access to affordable treatment.[6–8] It is one of the highest risk causes of mortality and cardiovascular disease across low-risk and high-risk population settings.[6,7] Clinically, earlier stage patients with CKD can be detected through laboratory screening by serum creatinine measurements, with effective treatments available to slow kidney failure and reduce cardiovascular events. Thus, the high prevalence and recommended approach for assessing CKD patients with high blood pressure and diabetic patients are through the standard urine dipstick test to detect the abnormal serum albumin levels (≤3.4 g/dL).[9] Even though the current point-of-care clinical diagnosis for CKD is by urine dipstick test, which has several drawbacks due to low sensitivity and frequently false negative or positive results.

Several techniques mentioned in publications, where analytical approaches can be utilized for detecting Albumin in urine samples, like enzyme-linked immunosorbent assay (ELISA), fluorescence immunoassay, immunoturbidimetric assay, radioimmunoassay, chip electrophoresis, and immunonephelometric.[10–12] Further, these techniques are more precise than the urine dipstick test. However, their examination approach remains weak due to complicated sample processing that necessitates longer handling time (ca. 5 h) for ELISA–labeling, polypeptides/proteins issue with fluorescence molecule by fluorescence immunoassay, which causes changes in the binding abilities of polypeptides/proteins once the fluorescence labels occupied the binding sites. Besides, the limit of detection (LOD) of radioimmunoassay of ca. 16 ng/mL necessitates protein labeled by a radioactive isotope. The rapid and easy approach by immunoturbidimetric assay thus necessitates a vast amount of antisera samples. Chip electrophoresis and immunonephelometric have greater sensitivity and accuracy while obliging to a high cost and massive machinery. Due to these restrictions, there is a necessity to develop an albumin assay that could address the above-mentioned issues and could be attested to a much easier, label-free, highly sensitive, and point-of-care for patients. Therefore, the Nano-structural PSCLCs smartphone-based biosensor was developed as an alternative method for albumin screening related to CKD. It is a smartphone-based biosensor combined with a smartphone to demonstrate the need to reduce the complicated systems or equipment. However, no study using ceramic silicon-constructed DMOAP to orientate Albumin in animal urine, combining a smartphone system in optical and biomedical applications. The developed PSCLCs smartphone-based biosensor was employed to detect the Albumin in urine samples as an alternative approach for future clinical CKD applications.

Materials and Methods

Materials and Preparation

The stabilized-CLCs mixtures were nematic LCs (E7, Merck) and chiral dopant (2.9 wt.%, R5011, Merck). A photocurable monomer (RM257, Merck) and photo-

initiator (DAROCUR-1173, Ciba) were also used. The sensitive interfacial effects between the CLCs molecules and the alignment layer of ceramic silicon-constructed DMOAP were used to detect bovine serum albumin (BSA). The PSCLCs smartphone-based biosensor schematic is demonstrated in Figure 1.

Initially, the CLCs molecules were allied near the substrates vertically with the ceramic silicon-constructed DMOAP coating. Also, the polymer networks assist the stabilization of the CLCs structure. Thus, with the firmly self-assemble features of the CLCs in intermediate space and interface effect of ceramic silicon-constructed DMOAP near the substrate, the CLCs molecules near the surfaces and the bulk region exhibit the focal conic (FC) and planar (P)-state, respectively. The function of the BSA concentration-dependent color change is caused by the changes in the arrangement of CLCs. Once the biomolecules or biomarkers are adsorbed onto the ceramic silicon-constructed DMOAP-coated substrates, the vertical anchoring force is weakened. Thus, the biomolecules allow the CLCs molecules to change into the P-state on the ceramic Silicon constructed DMOAP-coated substrate. The CLCs structure is transiting from the FC- to the P-state lead to the color-indicating characteristic of PSCLC devices. To prepare the PSCLC biosensor, the substrate was permeated in the ceramic silicon-constructed DMOAP aqueous solution for 15 min to coat the glass substrate's alignment layer. Next, the substrate was cleaned with deionized water to remove excess ceramic silicon-constructed DMOAP solution for 1 min. The test BSA was immobilized and fulfilled by the ceramic silicon-constructed DMOAP-coated glass in aqueous BSA solutions at 1 mg/mL, 1 µg/mL, and 1 ng/mL for 30 min. The unbound BSA was rinsed with DI water. Finally, each substrate was assembled with 11 µm spacers to form a sandwiched device. The assembly PSCLC biosensor with two biomolecules immobilized DMOAP-coated substrates are employed. The empty LC sandwiched cell was filled with PSCLCs by capillary action to create a PSCLC biosensor. To polymerize the monomer, the CLCs cell was irradiated with ultraviolet light at 350–380 nm. The curing time and intensity was 10 min and 5 mW/cm,^{2} respectively.

Instruments and System Design

The transmission spectra of the PSCLC device were measured by the high-resolution fiber optic spectrometer (Ocean Insight, HR2000+). Further, a smartphone was mounted on the stage, and the smartphone camera is aligned with a set of lenses embedded in the designed stage. Additionally, the sample device tray was designed to hold the PSCLCs cell in front of the lens. The sandwiched sample device tray was between two cover glasses (22 mm × 22 mm and 130 µm thick) with a parafilm spacer. To decrease the chromatic and spherical aberrations, an achromatic lens set composition, consisting of

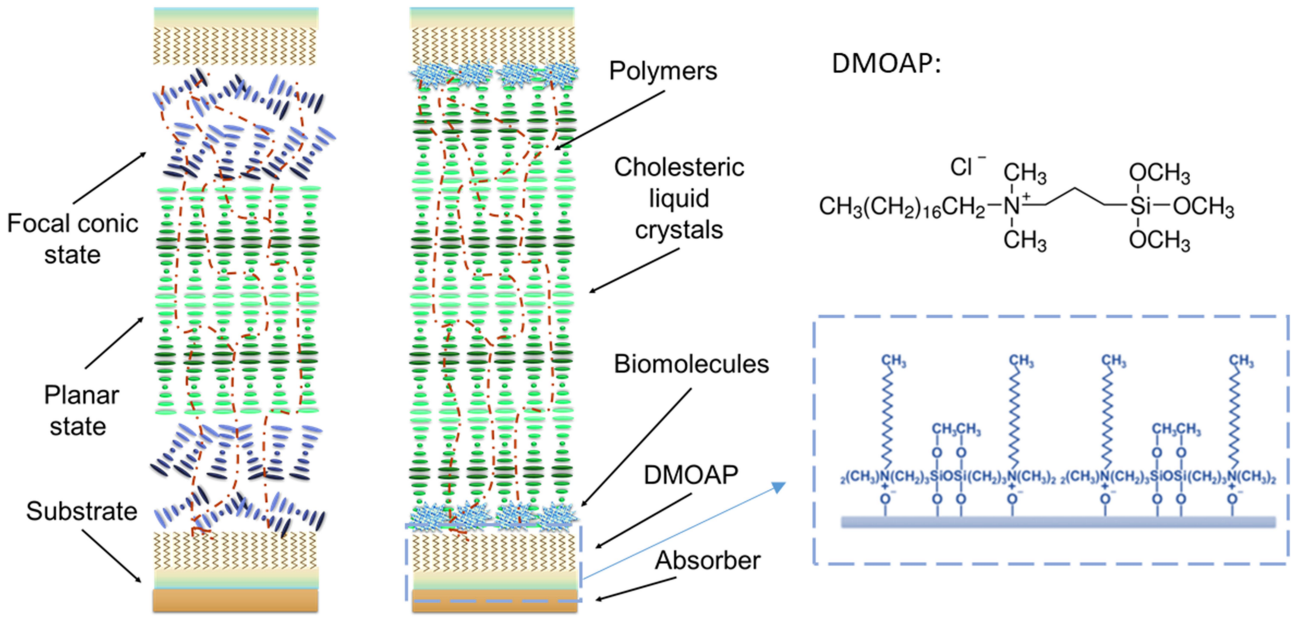

Figure 1 Schematic of the polymer-stabilized cholesteric structure biosensor. The configuration changes from the focal conic (FC)-planar (P)-FC to the P mode in the presence of biomolecules on the ceramic silicon-constructed DMOAP substrate.
Abbreviation: DMOAP, N,N-dimethyl-n-octadecyl-3- aminopropyltrimethoxysilyl chloride.

both dual-convex and concave-plane lens, was applied for measuring and imaging the PSCLCs texture. Figure 2A and B demonstrate the achromatic lens set by its less aberration than the simple dual-convex lens. In this new design system, the PSCLC biosensor was imaged through a magnification (5X) achromatic lens with a 10 mm diameter and a focal length of 4 mm, as confirmed by a calibration ruler. A photograph of PSCLC sample taken with a smartphone (OPPO), as shown in Figure 2C. The color-dependent on various BSA concentrations and oily streaks of CLCs could be seen clearly from the smartphone's camera screen (Figure 2D). The smartphone 3X

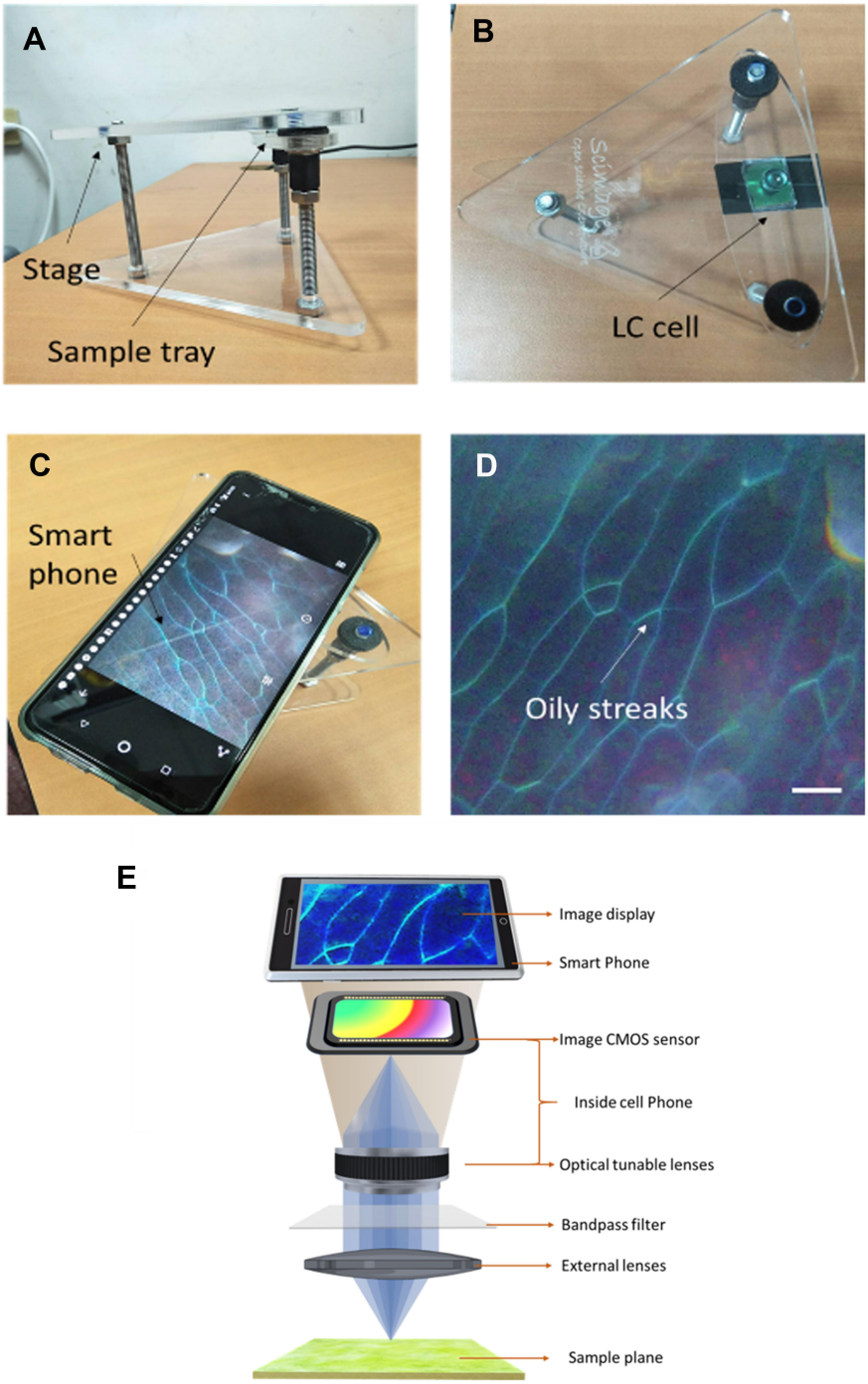

Figure 2 (**A**–**C**) Smartphone add-on system and setup of the optical system for PSCLCs biosensor chip, (**D**) oily streaks of CLC molecules from the camera of the smartphone in the system, and (**E**) the optical system setup. (Scalebar = 100 μm).
Abbreviation: LC, liquid crystal.

optical zoom lens camera to record in real-time color changes of the PSCLCs. The achromatic lens set with less aberration (Figure 2E).

In vivo Studies

Adult normal male Wistar rats were obtained from the BioLASCO Co. (Taipei, Taiwan). Approval for the in vivo investigation regarding rat's urine was acquired from the Institutional Animal Care and Use Committee at Taipei Medical University. All experiment processes were carried out based on the protocols approved by the Institutional Animal Care and Use Committee (IACUC) of Taipei Medical University (IACUC Approval protocol numbers: LAC-2018-0115; LAC-2020-0320). All experimental procedures were conducted in compliance with the "Guide for the Care and Use of Laboratory Animals", which was stipulated by the Institute of Laboratory Animal Resources, National Research Council, and published by the National Academy Press in 1996. The urine samples were collected from a male Wistar rat and added to the designated BSA concentration. As previously mentioned above, the developed PSCLC technology was used to detect the urine BSA in mimicking the clinical patient urine albumin.

Results

PSCLCs Smartphone-Based Biosensor Optical Textures

The optical textures for various BSA concentrations obtained from the smartphone camera are projected in Figure 3. As observed, the image's brightness increases, and defects on the oily streaks decrease with increased BSA concentrations. Thus, the light scattering induced by the random CLCs molecule called the FC-state is produced at lower BSA concentrations. Also, the number of oil defects in the textures was decreased with an increase in BSA concentration. The temperature-independent chiral dopant material R5011 was used in this report.[13] Therefore, the CLCs structure pitch is not thermosensitive, and the PSCLC biosensor can be employed in a wide range of temperatures conveniently. The PSCLC biosensors immobilized with different BSA concentrations at 0–10 mg/mL is also displayed in Figure 3.

The PSCLC biosensor produced different reflected colors at different BSA concentrations. However, the reflected PSCLC biosensor green color depicts the absence of BSA. Further, the color shift to blue with increasing concentrations of the BSA. The ceramic silicon-constructed DMOAP-coated glass aligned with LCs molecules homeotropically to produce the FC-states of the PSCLCs. Therefore, it possesses the potential to measure the amount of biomolecules with a logarithmic scale by color indication property of PSCLCs from a smartphone. The PSCLC structure aids the color variations and power reflected from the biosensors. The lower reflective FC/P/FC-state to a higher reflective P-state due to BSA and PSCLC molecules' interactions is also demonstrated in Figure 3. The number of biomolecules could be easily identified based on the color indication due to the PSCLC biosensors' color changes.

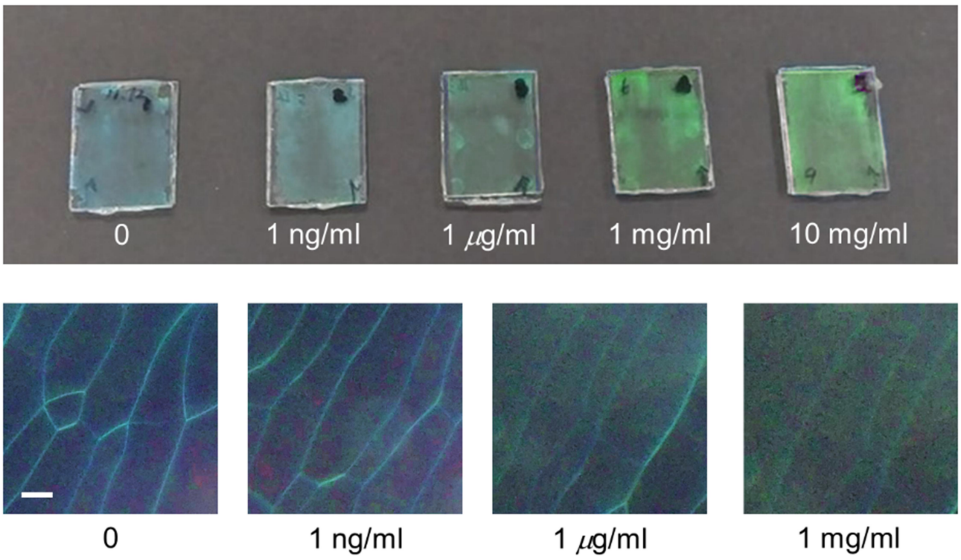

Figure 3 Color-indicating properties of PSCLCs biosensors in various BSA concentrations. Optical microscopic images of PSCLCs cells under various BSA concentration immobilized on the substrates (0–1 mg/mL). (Scalebar = 100 μm).

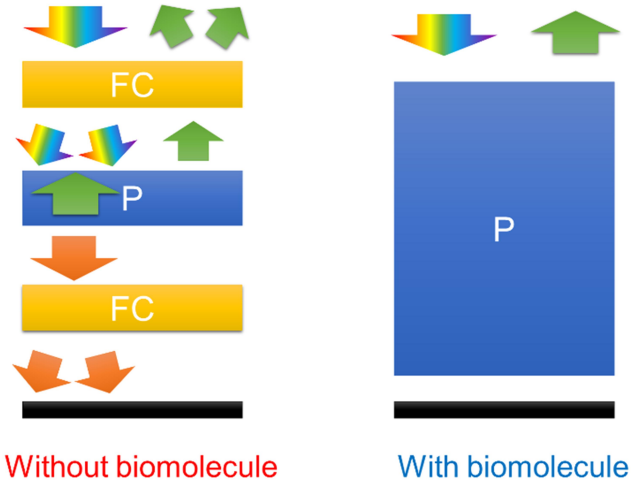

Figure 4 The mechanism of the PSCLCs biosensor in a situation with and without biomolecules.
Abbreviations: FC, focal conic; P, planar.

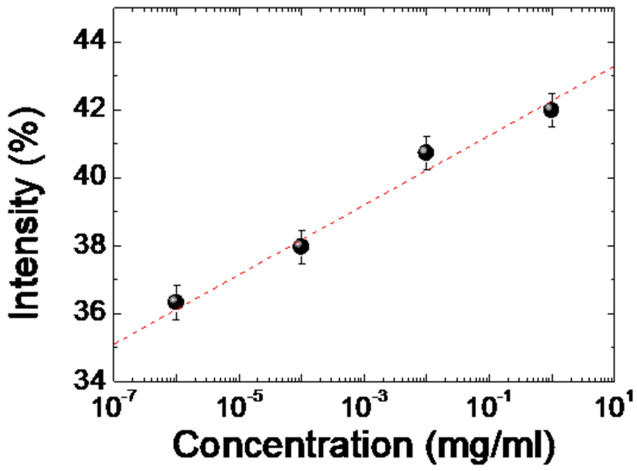

Figure 5 The correlations of the intensity from image software integration of a PSCLCs biosensor in various BSA concentrations (10^{-6}, 10^{-4}, 10^{-2}, and 1 mg/mL).

PSCLCs Biosensing Mechanism

The PSCLCs biosensing mechanism with and without biomolecules is shown in Figure 4. The immobilized BSA diminished the homeotropically anchoring power of the ceramic silicon-constructed DMOAP alignment layer. The CLC molecules changes to a P-state with increasing BSA concentrations, reflecting a near-perfect P-state of the PSCLC biosensors to exhibit a highly meditative state (Figure 4).

The incident light with the same handedness as the chirality of the PSCLC molecules will be reflected. The selective reflection (Bragg reflection) is induced in the spectral range:

$\lambda_0 = (n_e + n_o) \bullet P/2$,

where P is the pitch length of the helix in PSCLCs. The extraordinary refractive index (n_e) and the ordinary refractive index (n_o) were used. The selective Bragg reflection band in a PSCLCs device is centered at λ_0. Thus, if the Bragg reflection is in the visible range, the PSCLC device will reflect the colors at around 515 nm (green color). The lower and higher reflective modes of PSCLCs make the color reflection become differently. Based on the intensity and color reflection changes, the sensitivity of the PSCLC biosensor is achieved.

PSCLCs Quantitation Analysis

To achieve a quantitative experimental for the PSCLC biosensors, quantifying the PSCLC texture from the smartphone by software (ImageJ) with quantitation brightness function was employed.[14] The reflection intensity correlations of the biosensor at various BSA concentrations are displayed in Figure 5. The higher intensity was achieved with increasing BSA concentrations. A roughly logarithmic scale detection can successfully be achieved with a smartphone-based system. The approximately linear relationship between the optical intensity from image software quantitation pixels of the PSCLC biosensor and various BSA concentrations is proposed. Based on the quantitation of the intensities from the images achieved by the smartphone, a successful demonstration thus reflects that the smartphone can replace the expensive microscopy or spectrometer. Therefore, the PSCLCs smartphone-based biosensors will significantly increase the possibility of home use. Besides, details of detection properties can also be proposed using transmission spectra. The spectra of the PSCLC biosensors immobilized with different BSA concentrations are demonstrated in Figure 6. The light transmittance increased of the PSCLC biosensors, and the bandwidth of the Bragg reflection decreased with a rising BSA concentration.

When the biomolecules are adsorbed onto DMOAP-coated substrates, the vertical anchoring power is weakened. These biomolecules allow PSCLC molecules to transfer to the P-state. The PSCLC structure transiting from the FC to P mode brings the reflection property more obvious. The bandwidth is defined as the interval between 50% of the maximum transmittance of two band edges. Also, the LOD of the PSCLCs was near 1 ng/mL.

Moreover, the spectral change is not apparent when the BSA concentration is lower than 1 ng/mL. The PSCLC structure in the BSA vicinity on the substrate was the FC-phase at lower BSA concentrations. Therefore, the scattering light property undermined the band reflection of the CLCs. The clear P-state of CLCs was predominant when the BSA concentration is increased. The Bragg reflection photonic bandgap could be observed, which was more integrated

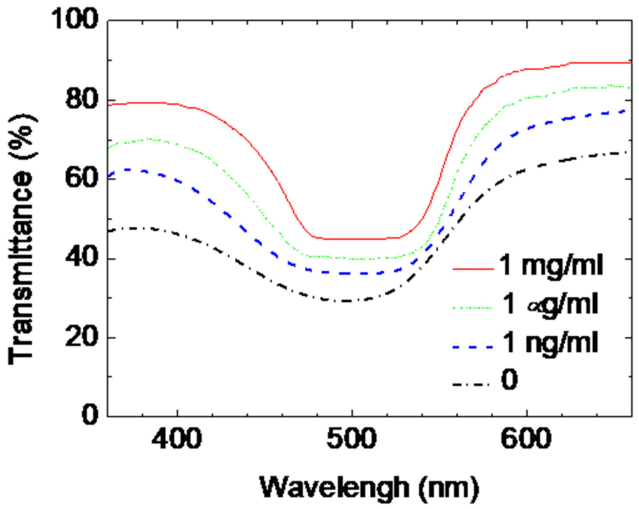

Figure 6 Transmission spectra of PSCLCs biosensor prepared with 0–1 mg/mL of BSA concentrations.

with rising BSA concentrations. Due to these properties, a logarithmic-scale PSCLC biosensor was demonstrated.

The transmittance correlation and Bragg reflection bandwidth of various BSA concentrations is displayed in Figure 7. The results demonstrated that the band reflection (Bragg reflection) of PSCLCs in the spectrum measurement could also be employed to quantitate and detect biomolecules in a linearized semi-log plot manner, with error bars (n = 10).

PSCLCs Immunoassay Analysis

The immunoassay experiment was designed to quantify and evaluate the PSCLC biosensor suitability functionality in clinical applications. It was examined with the use of BSA and anti-BSA antibody. The light intensities of the immunoassay PSCLCsdevices are immobilized with 0–10 μg/mL concentrations of BSA, and 0–1000 μg/mL concentrations of anti-BSA are shown in Figure 8. To assess the PSCLCs cell for BSA and immunocomplex of BSA pairs detection, the glass substrates were immersed in the aqueous solution containing 1.6% (v/v) DMOAP at ambient temperature to induce DMOAP-coated substrates. Later, followed by the anti-BSA immobilization on the glass substrates. The BSA antigen was reacted with anti-BSA to form the immunocomplex pair. Each substrate was assembled to form the PSCLC device with a 10-μm spacer.

The BSA antibody was mixed with identical BSA antigen concentrations to make the immunocomplexes between the specific antigen/antibody pairs. It is found that the lower concentrations of <10 μg/mL of the anti-BSA for the immunocomplexes could not easily compose the antigen/antibody mixtures. Thus, the light intensities of the 1 and 10 μg/mL concentrations of BSA do not increase. The BSA immunocomplex of antigen/antibody pairs induced a brighter P-state once the 100 with 1000 μg/mL of the anti-BSA were used under cross-polarized optical microscopy. However, the excessed concentration of the anti-BSA will significantly affect the PSCLC arrangement, which can intensify the difference of BSA immunocomplexes to be unidentified. This effect could cause a higher light intensity of BSA at the initial concentration. Therefore, higher anti-BSA concentrations cannot be used in the LCs system for immunoassay experimental. The quantitation for immunoassay results proves that BSA immunocomplexes can be used for the PSCLC system due to the disruption of the PSCLC arrangement. The anti-BSA with 1 μg/mL concentration was deemed suitable for the PSCLC device based on the data. The

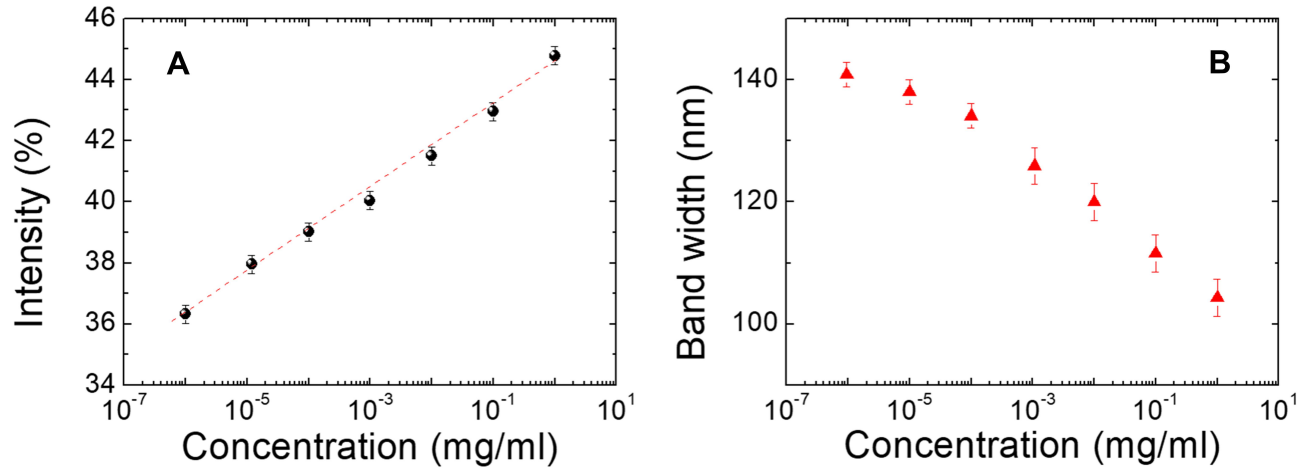

Figure 7 (**A**) The correlations of the minimum transmittance of Bragg's reflection at different BSA concentrations, and (**B**) correlations of the bandwidth of Bragg's reflection of PSCLCs biosensor at different BSA concentrations.

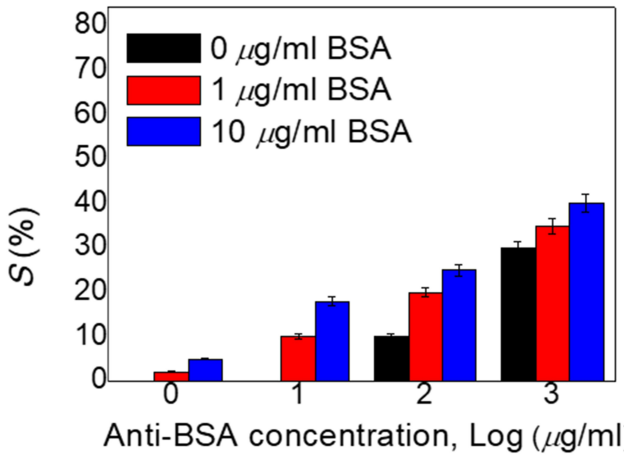

Figure 8 Intensities of immunoassay PSCLCs immobilized with BSA concentrations of 0, 1, and 10 μg/mL as well as 0, 10, 100, and 1000 μg/mL of anti-BSA concentrations.

PSCLC biosensor for immunodetection could be successfully displayed. The immunocomplexes could be detected in a lower concentration range through high-Δn LCs.[15] The significantly higher sensitivity in immunocomplexes was shown, and the LOD can be improved in the immunoassay PSCLCs system. As a result, the BSA in rat' urine can be detected based on this LCs technology (Figure 9A and B) and applied to detect BSA in animal urine. The photograph of preclinical animal urine collection is shown in Figure 9A. Additionally, the correlations of the transmittance at different BSA concentrations are shown in Figure 9B. The linear correlation between BSA concentrations of 0–2 mg/mL was shown in Figure 9B. Our results demonstrate that the optical anisotropy of PSCLCs can be utilized to establish a PSCLCs-based biosensing technique for potential preclinical urine quantitation.

Discussion

The novel PSCLC biosensor was demonstrated for measuring and quantifying biomolecules. The CLCs molecule's chirality is highly sensitive to BSA concentration on the ceramic silicon-constructed DMOAP alignment layer, with color changes observed through a smartphone camera. The quantitative approach for correlating intensity with BSA concentration has also been demonstrated with the LOD of the PSCLC biosensor close to 1 ng/mL, close to the commercial biosensor. Compared with previous work, the new label-free PSCLC biosensor could prove a sensitive and inexpensive platform for sensing, measuring biomolecules based on the color indication on a smartphone. Based on the spectra changes, the PSCLC biosensor immobilized with different BSA concentrations shows that the transmittance is increased. The bandwidth of the Bragg reflection decreased with a higher BSA concentration. The polymer network in PSCLCs could maintain the sensing performance of CLCs with minimal impact on the sensing performance. The immunodetection

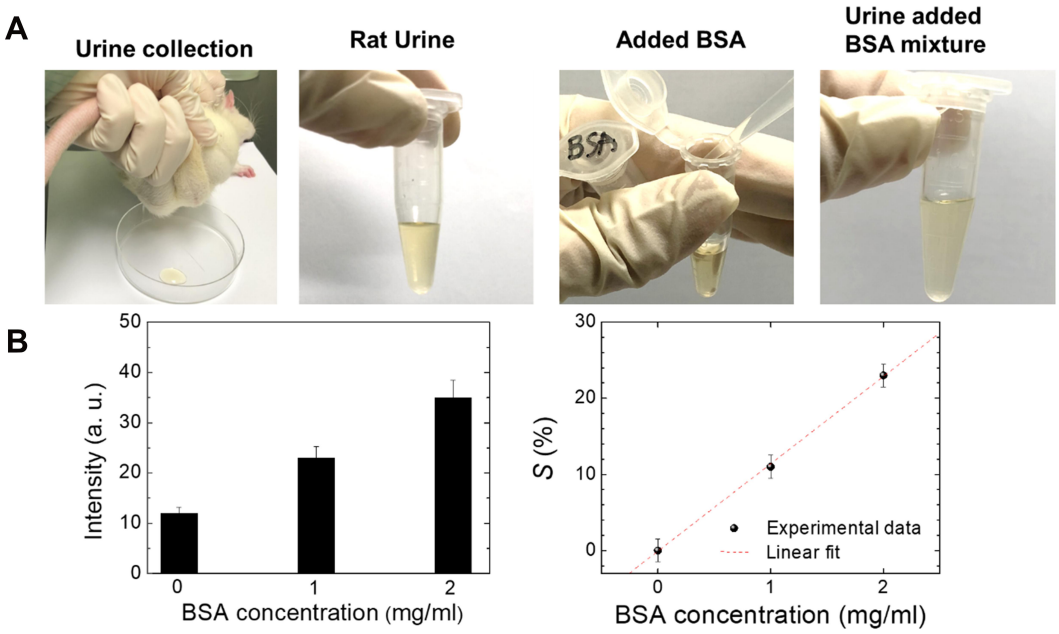

Figure 9 (**A**) Photograph of preclinical animal urine collection and BSA addition, and (**B**) detection of BSA in urine according to the developed LCs technology.
Abbreviation: BSA, bovine serum albumin.

could be successfully displayed with a 1 μg/mL concentration of suitable anti-BSA concentration.

Furthermore, the Label-free biosensing technique of the plasmonic and GCI was proposed in the past.[16–19] However, the problem of plasmonic and GCI sensors is the complicated measurement approach. Also, these devices are costly and immobile (unportable), which limits their practical realization. Compared with plasmonic and GCI sensors, our label-free PSCLC biosensor is cheaper, the same detection order as existing methods, and can be measured with a smartphone in a rough or detailed spectrum. Based on the color indications, the label-free nature, and facile manufacture shows these CLCs have the potential for development as a sensitive, cheap, color-indicating, smartphone-based biosensing technique. Compared to existing label-free techniques, the color-indicating LCs bioinspired sensor can be used as a microfluidic immunoassay application.[20]

The LCs biosensors as vital sensing technology,[2–4] initially concepts using biomolecules immobilized on the alignment film to make the reorientation (vertical-to-planar) of LCs molecules.[2] As a response to the reorientations, intensity changes of the transmitted light passing through LCs biosensor can be detected under cross-polarized optical microscopy.[21] Recently, LCs-established sensing techniques have been used to detect a wide range of targets, such as BSA, enzymatic reactions, antibody-antigen immunoreactions, the CA125 cancer biomarker, and DNA.[1–3,15,22–24] Their selectivity and specificity issues are solved by the antibody–antigen immunoreaction method.[23] The attractive nematic LCs/aqueous interface to trigger an LCs reorientation was observed and proposed by Noonan and Price.[25,26] However, the present LCs-based biosensing techniques need assistants from complicated systems such as polarizers, spectrometers, and other equipment, limiting their convenience for the end-users and increasing the cost for a single measurement.

The LOD of albumin through this assay could be attained at very tiny level. However, anti-albumin is adsorbed physically onto the slide, lacking uniformity orientational. The immunobinding efficiency, along with the assay reproducibility, may affect the system. Additionally, it only presents the qualitative consequences, owing to its "all-or-nothing" feature. It could not be applied to quantify physiological urine samples with a wide range of concentrations. Therefore, addressing this concern, the developed PSCLCs system assay was quantified to detect Albumin in the physiological solution.

The CLCs unique optical properties, such as stability and Bragg reflection,[27,28] are observed. Thus, the selectively light reflection, where polarization has the same handedness as the chirality of CLC, could form the periodically helical structure of CLCs. Further exciting features of CLCs are their bistable states, P- and FC-states, which means that no power is required to maintain both P- and FC-states of CLCs.[29] According to these exciting characteristics of CLCs, numerous uses have been forthcoming, liked photonic crystal chips,[30–32] reflective displays,[33] and electro-optical devices.[34,35] Furthermore, Hsiao et al 2015[5] investigated the sensitive and quantitative CLCs biosensor with color-indicating describing in detail the mechanism of CLCs sensing biomolecules up the possibility of CLCs as a new biosensor.[36] Table 1 shows the detection limits of several LC-based protein assays.[36–38] The BSA concentration range detected by our PSCLCs-based protein assay (1 ng/mL – 2 mg/mL) was closed to the same order of magnitude of LC-based protein assays.

Table 1 The Detectable Ranges of Current Assays for Protein Quantitation

Type of Assay		Detectable Range
Absorbance-based assay	UV absorption Bradford BCA	10–50 μg/mL 125–1500 μg/mL 10–1500 μg/mL
Fluorescence-based assay	Quant-iT NanoOrange	0.5–4 μg/mL 10 ng/mL–10 μg/mL
LC-based assay	NLC CLC	0.01 ng/mL–10 μg/mL 1 fg/mL–1 mg/mL

Conclusions

The PSCLCs smartphone-based biosensor with ceramic silicon compound (trimethoxysilyl)–constructed DMOAP has tremendously demonstrated as label-free, point-of-care, and less complicated towards the biosensing of BSA in a different approach. Assisting the platform in detecting BSA concentrations with an aided achromatic microscopic add-on system for a smartphone-based, which could be found to reveal high-resolution images ease interpretations. The sequence of images can be applied to measure albumin concentrations in urine with ease. Our system could be highly considered as an alternative approached for commercial systems. However, further investigation of biomarkers is necessary to evaluate this system's potential application in nanomedicine approaches.

Author Contributions

All authors made a significant contribution to the work reported, whether that is in the conception, study design, execution, acquisition of data, analysis and interpretation, or in all these areas; took part in drafting, revising or critically reviewing the article; gave final approval of the version to be published; have agreed on the journal to which the article has been submitted; and agree to be accountable for all aspects of the work.

Funding

This work was financially supported by the Ministry of Science and Technology (MOST), Taiwan, under grant no. MOST 109-2636-E-038-001, 108-2221-E-038-017-MY3, 108-2320-B-038-061-MY3; Taipei Medical University–Wan Fang Hospital, Taiwan under the grant no. 109TMU-WFH-14.

Disclosure

The authors report no conflicts of interest in this work.

References

1. Kim S-R, Abbott NL. Rubbed films of functionalized bovine serum albumin as substrates for the imaging of protein-receptor interactions using liquid crystals. *Adv Mater*. 2001;13(19):1445-+. doi:10.1002/1521-4095(200110)13:19<1445::AID-ADMA1445>3.0.CO;2-9
2. Chen C-H, Yang K-L. Detection and quantification of DNA adsorbed on solid surfaces by using liquid crystals. *Langmuir*. 2010;26(3):1427–1430. doi:10.1021/la9033468
3. Clare BH, Abbott NL. Orientations of nematic liquid crystals on surfaces presenting controlled densities of peptides: amplification of protein-peptide binding events. *Langmuir*. 2005;21(14):6451–6461.
4. Xue CY, Yang KL. Dark-to-bright optical responses of liquid crystals supported on solid surfaces decorated with proteins. *Langmuir*. 2008;24(2):563–567.
5. Hsiao YC, Sung YC, Lee MJ, Lee W. Highly sensitive color-indicating and quantitative biosensor based on cholesteric liquid crystal. *Biomed Opt Express*. 2015;6(12):5033–5038.
6. Levey AS, Atkins R, Coresh J, et al. Chronic kidney disease as a global public health problem: approaches and initiatives - a position statement from Kidney Disease Improving Global Outcomes. *Kidney Int*. 2007;72(3):247–259.
7. Wang HD, Naghavi M, Allen C, et al. Global, regional, and national life expectancy, all-cause mortality, and cause-specific mortality for 249 causes of death, 1980-2015: a systematic analysis for the Global Burden of Disease Study 2015. *Lancet*. 2016;388(10053):1459–1544.
8. World-Kidney-Day. Chronic Kidney Disease. What is Chronic Kidney Disease? 2020. Available from: https://www.worldkidneyday.org/facts/chronic-kidney-disease/. Accessed January 15, 2021.
9. Feldman M, Soni N, Dickson B. Influence of hypoalbuminemia or hyperalbuminemia on the serum anion gap. *J Lab Clin Med*. 2005;146(6):317–320.
10. Bargnoux A-S, Barrot A, Fesler P, et al. Evaluation of five immunoturbidimetric assays for urinary albumin quantification and their impact on albuminuria categorization. *Clin Biochem*. 2014;47(16–17):250–253. doi:10.1016/j.clinbiochem.2014.07.014
11. Krämer BK, Jesse U, Ress K, Schmülling R, Risler T. Enzyme-linked immunosorbent assay for urinary albumin at low concentrations. *Clin Chem*. 1987;33(4):609–611. doi:10.1093/clinchem/33.4.609
12. Wu -Y-Y, Yu W-T, Hou T-C, et al. A selective and sensitive fluorescent albumin probe for the determination of urinary albumin. *Chem Commun (Camb)*. 2014;50(78):11507–11510. doi:10.1039/C4CC04236K
13. Liu Y-J, Wu P-C, Lee W. Spectral variations in selective reflection in cholesteric liquid crystals containing opposite-handed chiral dopants. *Mol Crystals Liquid Crystals*. 2014;596(1):37–44. doi:10.1080/15421406.2014.918301
14. Hsiao Y-C. Liquid crystal-based tunable photonic crystals for pulse compression and signal enhancement in multiphoton fluorescence. *Opt Mater Express*. 2016;6(6):1929–1934. doi:10.1364/OME.6.001929
15. Sun S-H, Lee M-J, Lee Y-H, Lee W, Song X, Chen C-Y. Immunoassays for the cancer biomarker CA125 based on a large-birefringence nematic liquid-crystal mixture. *Biomed Opt Express*. 2015;6(1):245–256. doi:10.1364/BOE.6.000245
16. Abdulhalim I. Plasmonic sensing using metallic nano-sculptured thin films. *Small*. 2014;10(17):3499–3514. doi:10.1002/smll.201303181
17. Abdulhalim I. Optimized guided mode resonant structure as thermo-optic sensor and liquid crystal tunable filter. *Chinese Optics Letters*. 2009;7(8):667–670. doi:10.3788/COL20090708.0667
18. Kozma P, Hamori A, Cottier K, Kurunczi S, Horvath R. Grating coupled interferometry for optical sensing. *Appl Phys B Lasers Optics*. 2009;97(1):5–8. doi:10.1007/s00340-009-3719-1
19. Kozma P, Hamori A, Kurunczi S, Cottier K, Horvath R. Grating coupled optical waveguide interferometer for label-free biosensing. *Sensors and Actuators B: Chemical*. 2011;155(2):446–450. doi:10.1016/j.snb.2010.12.045
20. Fan Y-J, Chen F-L, Liou J-C, et al. Label-free multi-microfluidic immunoassays with liquid crystals on polydimethylsiloxane biosensing Chips. *Polymers (Basel)*. 2020;12(2):395. doi:10.3390/polym12020395
21. Gupta VK. Optical amplification of ligand-receptor binding using liquid crystals. *Science*. 1998;279(5359):2077–2080. doi:10.1126/science.279.5359.2077
22. Su H-W, Lee Y-H, Lee M-J, Hsu Y-C Y-C, Lee W. Label-free immunodetection of the cancer biomarker CA125 using high-Δn liquid crystals. *J Biomed Opt*. 2014;19(7):077006. doi:10.1117/1.JBO.19.7.077006
23. Su HW, Lee MJ, Lee W. Surface modification of alignment layer by ultraviolet irradiation to dramatically improve the detection limit of liquid-crystal-based immunoassay for the cancer biomarker CA125. *J Biomed Opt*. 2015;20(5):57004.
24. Wong TS, Chen TH, Shen X, Ho CM. Nanochromatography driven by the coffee ring effect. *Anal Chem*. 2011;83(6):1871–1873.
25. Noonan PS, Roberts RH, Schwartz DK. Liquid crystal reorientation induced by aptamer conformational changes. *J Am Chem Soc*. 2013;135(13):5183–5189.
26. Price AD, Schwartz DK. DNA hybridization-induced reorientation of liquid crystal anchoring at the nematic liquid crystal/aqueous interface. *J Am Chem Soc*. 2008;130(26):8188–8194.
27. Wang L, Dong H, Li Y, et al. Luminescence-driven reversible handedness inversion of self-organized helical superstructures enabled by a novel near-infrared light nanotransducer. *Adv Mater*. 2015;27(12):2065–2069.
28. Wang Y, Li Q. Light-driven chiral molecular switches or motors in liquid crystals. *Adv Mater*. 2012;24(15):1926–1945.
29. Hsiao YC, Tang CY, Lee W. Fast-switching bistable cholesteric intensity modulator. *Opt Express*. 2011;19(10):9744–9749.
30. Hsiao YC, Hou CT, Zyryanov VY, Lee W. Multichannel photonic devices based on tristable polymer-stabilized cholesteric textures. *Opt Express*. 2011;19(24):23952–23957.
31. Hsiao YC, Wu CY, Chen CH, Zyryanov VY, Lee W. Electro-optical device based on photonic structure with a dual-frequency cholesteric liquid crystal. *Opt Lett*. 2011;36(14):2632–2634.

32. Hsiao YC, Zou YH, Timofeev IV, Zyryanov VY, Lee W. Spectral modulation of a bistable liquid-crystal photonic structure by the polarization effect. *Opt Mater Express*. 2013;3(6):821–828.
33. Hsiao YC, Lee W. Polymer stabilization of electrohydrodynamic instability in non-iridescent cholesteric thin films. *Opt Express*. 2015;23(17):22636–22642.
34. Hsiao YC, Lee W. Lower operation voltage in dual-frequency cholesteric liquid crystals based on the thermodielectric effect. *Opt Express*. 2013;21(20):23927–23933.
35. Hsiao YC, Lee W. Electrically induced red, green, and blue scattering in chiral-nematic thin films. *Opt Lett*. 2015;40(7):1201–1203.
36. Chen FL, Fan YJ, Lin JD, Hsiao YC. Label-free, color-indicating, and sensitive biosensors of cholesteric liquid crystals on a single vertically aligned substrate. *Biomed Opt Express*. 2019;10(9):4636–4642.
37. Ernst O, Zor T. Linearization of the bradford protein assay. *J Vis Exp*. 2010;38:e1918.
38. Spence MT, Johnson ID. *The Molecular Probes Handbook: A Guide to Fluorescent Probes and Labeling Technologies*. Univerza v Ljubljani, Fakulteta za farmacijo; 2010.